# Global Scaling of Operational Modal Analysis Modes with the OMAH Method

A. Brandt

*University of Southern Denmark, Department of Technology and Innovation*
*Campusvej 55, DK-5230 Odense M, Denmark - email: abra@iti.sdu.dk*

M. Berardengo

*Università degli Studi di Parma, Department of Engineering and Architecture,*
*Parco Area delle Scienze, 181/A - 43124 Parma, Italy - email: marta.berardengo@unipr.it*

S. Manzoni

*Politecnico di Milano, Department of Mechanical Engineering,*
*Via La Masa, 34 - 20156 Milan, Italy - email: stefano.manzoni@polimi.it*

M. Vanali

*Università degli Studi di Parma, Department of Engineering and Architecture,*
*Parco Area delle Scienze, 181/A - 43124 Parma, Italy - email: marcello.vanali@unipr.it*

A. Cigada

*Politecnico di Milano, Department of Mechanical Engineering,*
*Via La Masa, 34 - 20156 Milan, Italy - email: alfredo.cigada@polimi.it*

**Abstract**

Modal models from operational modal analysis (OMA) lack information about
the modal scaling (or, modal mass). Many times, this is not a limitation. How-
ever, in some engineering applications, e.g. for structural health monitoring
or computational model validation, a scaled modal model may be important.
The authors of this paper recently presented a new approach for scaling modal
models using harmonic excitation. The method was named the OMAH method,
and it was shown that the approach is robust and reliable. However, the pro-
posed technique relied on the measurement of the structural response between
two arbitrary degrees of freedom (DOFs) for each mode. In the present paper,

*A. Brandt
*Email address:* abra@iti.sdu.dk (A. Brandt)

the method is extended to the case in which several excitation and response DOFs may be taken into account for the scaling. This is analogue to using global parameter estimation methods in classical experimental modal analysis. The proposed multiple-reference technique includes the capability of estimating residual terms to account for modes outside the frequency range of interest. The method is validated on two sets of data from real full scale structures, and the accuracy of the scaling using several response DOFs is shown to improve compared to using only a single excitation and response DOF. The proposed formulation, furthermore, allows one or more excitation DOFs as well as one or more response DOFs to be used for the scaling of the modal model. Thus, one single formulation can be used regardless of whether multiple-references are necessary, or not.

## 1. Introduction

Modal analysis is a powerful tool to estimate modal parameters of mechanical structures and systems. The knowledge of eigenfrequencies and mode shapes is crucial for many purposes: e.g., model validation and calibration, response estimation, and structural health monitoring. In many cases, the modal model must be properly scaled. This is one of the main limitations of operational modal analysis (OMA), which only provides unscaled modal models, because the loads acting on the structure are not known (e.g. [1, 2, 3, 4, 5, 6]).

There are different approaches available in the literature for scaling the modal model provided by OMA. Some of them require to repeat the OMA tests with different configurations of the structure. This means to change, in a controlled way, the distribution/amount of the mass or stiffness of the structure [7, 8, 9, 10, 11, 12, 13, 14, 15, 16, 17, 18, 19]. Another approach is the technique called *operational modal analysis with exogenous inputs* (OMAX). This method is based on the excitation of the structure being partly provided by natural en-

2

vironmental excitation (e.g. traffic, wind) and partly by one or more actuators providing measured broadband excitation [20, 21]. Further techniques couple known dynamic systems (e.g. people, tuned mass dampers) to the structure under investigation. This enables to estimate the modal masses and thus to scale the mode shapes [22, 23, 24]. Using cepstrum analysis to find the poles and zeros of the system is another approach, although this method relies on *a priori* knowledge of at least one system frequency response [25]. Finally, the mass matrix of a finite element model may be used, together with expanded experimental mode shapes, to find the modal masses [26].

All the approaches mentioned above require accurate knowledge of the dynamics of additional systems, or require to employ potentially large actuators (on large structures) capable of producing broadband excitation signals (e.g., multi-harmonic, chirp), or rely on relatively complicated experimental procedures (e.g. changes of distribution/amount of the mass of the structure), or, again, rely on the accuracy of a computational model, which latter must be based on an assumption. Recently, the authors of the present paper proposed a new approach to scale modes estimated by means of OMA by employing mono-harmonic excitation [27, 28]. This approach, named OMAH, was shown to be robust and reliable. Furthermore, the estimation of the harmonic responses under different signal-to-noise ratios (SNR) using the three-parameter sine fit method was investigated in [29]. Here it was shown that it is a particular advantage with harmonic excitation, that it can provide high accuracy also in cases with poor SNRs. This means the method can be employed using relatively small actuators.

The present paper explains how to improve the accuracy of the scaling procedure. This is accomplished by increasing the number of degrees-of-freedom (DOFs) in which the response to the mono-harmonic excitation is measured. Moreover, this extension of the method also allows data from additional excitation DOFs to be used, which may be necessary when a single excitation DOF cannot be used to excite all modes of interest.

The layout of the paper is as follows: Section 2 first presents the theory

3

related to this work as well as the OMAH method introduced in [27, 28]; then it introduces the method for global scaling of the modal model, to improve the accuracy of the scaling procedure, including residual terms, if so desired; Section 3 presents experimental tests carried out and discusses the validation of the proposed global scaling of OMA modes.

## 2. Theoretical background

In this section we first discuss the theory behind the OMAH method (see Section 2.1), which is the base for the new approach proposed here for the global scaling. Then, the new, global approach is presented and discussed in detail (see Section 2.2).

### 2.1. The OMAH method

A scaled frequency response function (FRF) of a structure can be formulated generally in receptance form (displacement over force) as:

$$H_{p,q}(\mathrm{j}\omega) = \sum_{r=1}^{N} \frac{\psi_r^p \psi_r^q Q_r}{(\mathrm{j}\omega - s_r)} + \frac{(\psi_r^p \psi_r^q Q_r)^*}{(\mathrm{j}\omega - s_r^*)} \tag{1}$$

where $\omega$ is the angular frequency, $p$ is the DOF where the structural response is measured while $q$ is the DOF where excitation is provided. Furthermore, $s_r$ is the pole of mode $r$ and the superscript $*$ denotes complex conjugation. $\psi_r^p$ and $\psi_r^q$ are the mode shape coefficients of mode $r$ at points $p$ and $q$, respectively. $N$ is the number of modes considered, j is the imaginary unit and, finally, $Q_r$ is the modal scaling constant of mode $r$. The expression of $s_r$ is:

$$s_r = -\zeta_r \omega_r + \mathrm{j}\omega_r \sqrt{1 - \zeta_r^2} \tag{2}$$

where $\omega_r$ and $\zeta_r$ are the eigenfrequency and non-dimensional damping ratio of mode $r$, respectively. The expression of $Q_r$ is:

$$Q_r = \frac{1}{2\mathrm{j}m_r\omega_r\sqrt{1 - \zeta_r^2}} \tag{3}$$

4

where $m_r$ is the modal mass of mode $r$.

Often (for example in the case of proportional damping), the expression provided in Equation (1) can alternatively be written as:

$$H_{p,q}(\mathrm{j}\omega) = \sum_{r=1}^{N} \frac{\psi_r^q \psi_r^p}{m_r(\mathrm{j}\omega - s_r)(\mathrm{j}\omega - s_r^*)} \tag{4}$$

In OMA, the poles and the values of $\psi_r^q$ and $\psi_r^p$ are obtained by the parameter extraction, and, according to Equation (4), scaling the modal model thus reduces to finding the modal mass, $m_r$, of the modes to be scaled.

OMAH allows to scale the modal model components by applying a measured mono-harmonic force in one DOF, at (or close to) each natural frequency of the modes to be scaled, and measuring the response in the same/another DOF. This single frequency measurement can then be used to obtain the scaling of the mode by assuming that a single mode is dominating at the excitation frequency considered, which will be equivalent to a single-degree-of-freedom (SDOF) approach [27]. However, also multi-degrees-of-freedom (MDOF) problems can be solved with an extension of the same approach [28].

The first part of OMAH is thus to carry out an OMA, finding the $s_r$ values and the corresponding unscaled mode shape components $\psi_r^p$, where $p$ indicates generic DOFs of the structure where its response has been measured during the OMA test. Then, the second part of the method consists of providing a measured mono-harmonic excitation (at one or more frequencies $\omega_{\mathrm{ex}}$ close to the natural frequency or frequencies $\omega_r$) to the structure in DOF $q$. It is essential that $q$ is a point where the structural vibration was acquired during the OMA test.

If a SDOF approximation of the structural dynamics is considered, the FRF of Equation (4) at $\omega_{\mathrm{ex}}$ can be approximated as:

$$H_{p,q}(\mathrm{j}\omega_{\mathrm{ex}}) \simeq \frac{\psi_r^q \psi_r^p}{m_r(\mathrm{j}\omega_{\mathrm{ex}} - s_r)(\mathrm{j}\omega_{\mathrm{ex}} - s_r^*)} \tag{5}$$

If $H_{p,q}(\mathrm{j}\omega_{\mathrm{ex}})$ is measured, the value of $m_r$ can be estimated as:

$$m_r = \frac{\psi_r^q \psi_r^p}{H_{p,q}(\mathrm{j}\omega_{\mathrm{ex}})(\mathrm{j}\omega_{\mathrm{ex}} - s_r)(\mathrm{j}\omega_{\mathrm{ex}} - s_r^*)} \tag{6}$$

5

If higher accuracy is required, or if there is high modal density so that several modes are contributing to the FRF at frequency $\omega_{\mathrm{ex}}$, then $H_{p,q}(\mathrm{j}\omega_{\mathrm{ex}})$ evaluated at several different frequencies $\omega_{\mathrm{ex}}$ can be used; at least as many frequencies as the number of modes to be scaled.

At least two more frequencies than the number of modes in the frequency range of interest should be excited to increase the accuracy. This allows for residual terms, accounting for the out-of-band modes, to be computed. The requested modal masses can then be computed by using a least squares solution. Even in the case of using several values of $\omega_{\mathrm{ex}}$, we propose using frequencies close to each eigenfrequency because this will require lower force excitation, and thus require a smaller, less expensive actuator. More details about OMAH are available in [27, 28, 30].
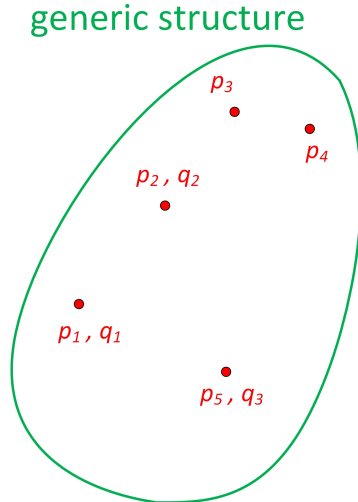
*2.2. Global scaling with the OMAH method*



Figure 1: A generic structure where structural response in OMAH tests is measured in 5 DOFs ($m$=5) and excitation is provided in 3 DOFs ($v$=3), illustrating that the indeces for the response and excitation DOFs do not necessarily agree. In this example, the two first excitation DOFs agree with the two first response DOFs, whereas the third excitation DOF, $q_3$, corresponds to response DOF $p_5$

The estimation of the modal masses with the original method described in Section 2.1 requires to use the values of $\psi_r^p$ and $\psi_r^q$ defined by the two DOFs of the FRF, $p$ and $q$. The OMA estimates of these two values are, of course, affected by uncertainty due to random errors in the correlation function estimates propagating through the OMA parameter extraction. Errors in the estimated values of $\psi_r^p$ and $\psi_r^q$ in turn affect the estimation of the modal mass $m_r$. The OMA estimates of the poles will, of course, also affect the estimation of modal mass, but will lead to a bias error which is not easily averaged away. The OMAH method, however, gives an easy opportunity to see if the natural frequency is accurately determined, by observing the phase relationship between force and response in the driving point. Thus, any errors in the pole estimate can be readily found and, if desired, corrected.

To reduce the variance in the estimates of modal masses, in the present paper we therefore propose to increase the number of DOFs used for the scaling. The driving idea is to measure the structural response in more than one DOF (i.e. $p_1, p_2, ..., p_m$) when applying the mono-harmonic excitation. All these DOFs must correspond to DOFs where the structural response was measured during the OMA test, so that there exists a mode shape coefficient for each DOF. We will also include the possibility of using FRFs from more than one excitation DOF (i.e. $q_1, q_2, ..., q_v$) (note that, with this notation, DOFs $p_n$ and $q_n$ are not necessarily the same DOFs: the number $n$ just indicates the $n$th DOF considered for the responses and the $n$th DOF considered for the inputs; see, as an example, Fig. 1), where DOFs $p_1$ and $p_2$ are the same as $q_1$ and $q_2$, respectively, but DOF $p_5$ is the same as $q_3$. Using more than one excitation DOF is necessary if a single excitation DOF cannot be found, which is not on a node line for any of the modes. In many OMA cases, all DOFs are not simultaneously measured, but rather acquired in batches. In such cases it may be natural to use the DOFs from one set of response DOFs that were used for the OMA test (most conveniently the last set, since these sensors are connected to the measurement system at the end of the OMA test, prior to scaling the modal model). In some cases, once the mode shapes are known, it may, however,

7

be desirable to optimize which DOFs to use for the scaling, by using only those DOFs with the largest mode shape coefficients.

We refer to the scaling method described here as *global scaling*, with reference to experimental modal analysis, where global modal parameter estimation methods are methods taking many DOFs into account for the parameter estimation.

We will formulate an equation system which can be solved by a least squares approach. Assuming we wish to scale a number $g$ of modes, starting from mode number $h$, the starting point is an arbitrary FRF, between the force in DOF $q$ and the response in DOF $p$, which can be written as:

$$H_{p,q}(\mathrm{j}\omega) \approx \sum_{r=h}^{h+g-1} \frac{\psi_r^p \psi_r^q}{m_r(\mathrm{j}\omega - s_r)(\mathrm{j}\omega - s_r^*)} + \frac{C_{pq}}{\omega^2} + D_{pq} \tag{7}$$

where $C_{pq}$ and $D_{pq}$ are residual terms accounting for the out-of-band modes.

We now assume that we have measured a number of FRFs, where $p = p_1, p_2, ..., p_m$, and $q = q_1, q_2, ..., q_v$. Furthermore, we have measured each individual FRF, $H_{p,q}(\mathrm{j}\omega)$, at one or more frequencies $\omega_{\mathrm{ex},1}, \omega_{\mathrm{ex},2}, \ldots, \omega_{\mathrm{ex},k}$. We put all those individual FRF values in a column vector:

$$\begin{aligned}
\mathbf{H}_\mathrm{l} = [&H_{p_1,q_1}(\mathrm{j}\omega_{\mathrm{ex},1}) \quad H_{p_1,q_1}(\mathrm{j}\omega_{\mathrm{ex},2}) \quad \ldots \quad H_{p_2,q_1}(\mathrm{j}\omega_{\mathrm{ex},1}) \quad H_{p_2,q_1}(\mathrm{j}\omega_{\mathrm{ex},2}) \quad \ldots \\
&H_{p_m,q_1}(\mathrm{j}\omega_{\mathrm{ex},1}) \quad H_{p_m,q_1}(\mathrm{j}\omega_{\mathrm{ex},2}) \quad \ldots \quad H_{p_1,q_2}(\mathrm{j}\omega_{\mathrm{ex},1}) \quad H_{p_1,q_2}(\mathrm{j}\omega_{\mathrm{ex},2}) \quad \ldots \\
&H_{p_m,q_v}(\mathrm{j}\omega_{\mathrm{ex},1}) \quad H_{p_m,q_v}(\mathrm{j}\omega_{\mathrm{ex},2}) \quad \ldots]^\mathrm{T}
\end{aligned} \tag{8}$$

where the superscript $[\ ]^\mathrm{T}$ denotes vector transpose.

We then define a column vector $\mathbf{x}_\mathrm{l}$ including the unknown modal masses and residual terms by:

$$\begin{aligned}
\mathbf{x}_\mathrm{l} = \Big[&\frac{1}{m_h} \quad \ldots \quad \frac{1}{m_{h+g-1}} \ldots \\
&C_{p_1 q_1} \quad D_{p_1 q_1} \quad C_{p_2 q_1} \quad D_{p_2 q_1} \ldots \\
&C_{p_m q_1} \quad D_{p_m q_1} \quad C_{p_1 q_2} \quad D_{p_1 q_2} \quad \ldots \\
&C_{p_m q_v} \quad D_{p_m q_v}\Big]^\mathrm{T}
\end{aligned} \tag{9}$$

For simplicity, we now introduce the function $\Gamma(p, q, r, \omega_{\text{ex}})$, defined by:

$$\Gamma(p, q, r, \omega_{\text{ex}}) = \frac{\psi_r^p \psi_r^q}{(j\omega_{\text{ex}} - s_r)(j\omega_{\text{ex}} - s_r^*)} \tag{10}$$

Using this function, we define the matrix $\mathbf{A}_l$, containing the mode contributions, and the coefficients $1/\omega_{\text{ex}}^2$ and $1$ in the positions for the residual terms:

$$\mathbf{A}_l = \begin{bmatrix}
\Gamma_{(p_1,q_1,h,\omega_{\text{ex},1})} & \Gamma_{(p_1,q_1,h+1,\omega_{\text{ex},1})} & \cdots & \Gamma_{(p_1,q_1,h+g-1,\omega_{\text{ex},1})} & 1/\omega_{\text{ex},1}^2 & 1 & 0 & 0 & \cdots \\
\Gamma_{(p_1,q_1,h,\omega_{\text{ex},2})} & \Gamma_{(p_1,q_1,h+1,\omega_{\text{ex},2})} & \cdots & \Gamma_{(p_1,q_1,h+g-1,\omega_{\text{ex},2})} & 1/\omega_{\text{ex},2}^2 & 1 & 0 & 0 & \cdots \\
\vdots & \vdots & \vdots & \vdots & \vdots & \vdots & \vdots & \vdots & \vdots \\
\Gamma_{(p_2,q_1,h,\omega_{\text{ex},1})} & \Gamma_{(p_2,q_1,h+1,\omega_{\text{ex},1})} & \cdots & \Gamma_{(p_2,q_1,h+g-1,\omega_{\text{ex},1})} & 0 & 0 & 1/\omega_{\text{ex},1}^2 & 1 & \cdots \\
\Gamma_{(p_2,q_1,h,\omega_{\text{ex},2})} & \Gamma_{(p_2,q_1,h+1,\omega_{\text{ex},2})} & \cdots & \Gamma_{(p_2,q_1,h+g-1,\omega_{\text{ex},2})} & 0 & 0 & 1/\omega_{\text{ex},2}^2 & 1 & \cdots \\
\vdots & \vdots & \vdots & \vdots & \vdots & \vdots & \vdots & \vdots & \vdots \\
\Gamma_{(p_m,q_1,h,\omega_{\text{ex},1})} & \Gamma_{(p_m,q_1,h+1,\omega_{\text{ex},1})} & \cdots & \Gamma_{(p_m,q_1,h+g-1,\omega_{\text{ex},1})} & & & \cdots & & \\
\Gamma_{(p_m,q_1,h,\omega_{\text{ex},2})} & \Gamma_{(p_m,q_1,h+1,\omega_{\text{ex},2})} & \cdots & \Gamma_{(p_m,q_1,h+g-1,\omega_{\text{ex},2})} & & & \cdots & & \\
\vdots & \vdots & \vdots & \vdots & \vdots & \vdots & \vdots & \vdots & \vdots \\
\Gamma_{(p_1,q_2,h,\omega_{\text{ex},1})} & \Gamma_{(p_1,q_2,h+1,\omega_{\text{ex},1})} & \cdots & \Gamma_{(p_1,q_2,h+g-1,\omega_{\text{ex},1})} & & & \cdots & & \\
\Gamma_{(p_1,q_2,h,\omega_{\text{ex},2})} & \Gamma_{(p_1,q_2,h+1,\omega_{\text{ex},2})} & \cdots & \Gamma_{(p_1,q_2,h+g-1,\omega_{\text{ex},2})} & & & \cdots & & \\
\vdots & \vdots & \vdots & \vdots & \vdots & \vdots & \vdots & \vdots & \vdots \\
\Gamma_{(p_m,q_v,h,\omega_{\text{ex},1})} & \Gamma_{(p_m,q_v,h+1,\omega_{\text{ex},1})} & \cdots & \Gamma_{(p_m,q_v,h+g-1,\omega_{\text{ex},1})} & & & \cdots & & \\
\Gamma_{(p_m,q_v,h,\omega_{\text{ex},2})} & \Gamma_{(p_m,q_v,h+1,\omega_{\text{ex},2})} & \cdots & \Gamma_{(p_m,q_v,h+g-1,\omega_{\text{ex},2})} & & & \cdots & & \\
\vdots & \vdots & \vdots & \vdots & \vdots & \vdots & \vdots & \vdots & \vdots
\end{bmatrix} \tag{11}$$

It is important to note that each row in $\mathbf{A}_l$, although indicated as the same frequencies $\omega_{ex,1}, \omega_{ex,2}$ etc., may actually have unique frequencies, since each row is an independent equation at an arbitrary frequency. Each row also contains one term $1/\omega_{\text{ex}}^2$, and one unity term, positioned for the appropriate residual terms, although they are not shown in the lowest rows of Equation (11).

Using the vectors and the matrix thus defined, the entire equation system with all the measured FRFs $H_{p,q}(j\omega)$ can be written as:

$$\mathbf{H}_l = \mathbf{A}_l \mathbf{x}_l \tag{12}$$

which can be solved by a least squares solution or a pseudo inverse.

9

In order to be able to solve Equation (12), first of all it needs to have more rows than the number of unknown modal masses plus residual terms, in order to be overdetermined. This will in general easily be accomplished if each mode is excited near its natural frequency, and several response points are used for each excitation frequency.

It should be noted that $\mathbf{x}_l \in \mathbb{R}^{(g+2(m \times v)) \times 1}$ and thus we need at least $(g + 2(m \times v))$ equations to solve the system. If we measure the structural response in all the response DOFs synchronously (i.e. we acquire $m$ responses for each excitation frequency $\omega_{\mathrm{ex}}$ and input DOF $q$), then the required value of $k$ (i.e. the number of the considered excitation frequencies) is $k \geq (g + 2(m \times v))/m$. Obviously, if $(g + 2(m \times v))/m$ is not an integer number, it must be rounded to the nearest higher integer number.

Furthermore, we need to make sure the matrix $\mathbf{A}_l$ is well conditioned. In general many of the values of the functions $\Gamma()$ are small numbers, since they are the contributions at frequency $\omega_{\mathrm{ex}}$ of each mode. As we assume each $\omega_{\mathrm{ex}}$ is a frequency close to one of the natural frequencies, then all coefficients $\Gamma()$ related to the modes considered, except the one related to the mode close to the excitation frequency, will, in most cases, be small. However, for the matrix $\mathbf{A}_l$ to be well conditioned, it is sufficient that each row and each column contains at least one large value, and that each row or column is unique. The condition for the columns is satisfied if each mode is well excited by at least one excitation DOF, $q$, in one of the rows, and measured by at least one response DOF with high mode shape coefficient, which is readily accomplished. For the rows, however, there is no guarantee that there is a high $\Gamma()$ value, since at one frequency, if the response DOF is on a node line for the corresponding mode at that frequency, all function values of $\Gamma()$ may be small, even if the excitation DOF is in a position exciting the mode well. The condition of the matrix is not affected by this, however, as there is a unity number in the position for the upper residual term. So, provided that each mode is well excited in at least one column of the matrix, then the matrix will be well conditioned. For this to be ensured, it is important that the residual terms are included in the definition

10

Table 1: Modal data of the staircase identified by means of OMA

| Mode | $\omega_r/(2\pi)$ [Hz] | $\xi_r$ [%] |
|:----:|:----------------------:|:-----------:|
| 1    | 7.84                   | 0.22        |
| 2    | 8.88                   | 0.39        |

of $\mathbf{A}_1$. We have not observed any significant difference in the accuracy by using different number of rows in the matrix $\mathbf{A}_1$, but as will be shown in Section 3.1, adding more rows with DOFs with a high response for the mode excited at the frequency in question, should add to the accuracy of the scaling.

It should also be mentioned that, in many cases where each mode is excited well by using one excitation DOF, it may be enough to use such an excitation DOF, and only a few response DOFs. These can then often be measured simultaneously at each frequency, and thus it may be sufficient to excite all modes at one frequency each, to provide enough rows so that the matrix is overdetermined and well conditioned.

The next section discusses the experiments carried out to validate what has been presented so far.

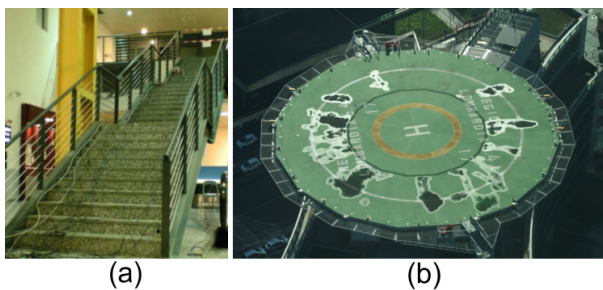## 3. Experimental tests



(a)          (b)

Figure 2: The tested structures: the staircase (a) and the helipad (credits: Wikimedia Commons) (b).

Two structures were used to validate the methods presented in Section 2.2. The first one is a staircase (12.03 m long, 1.80 m wide, and 5.22 m tall; made
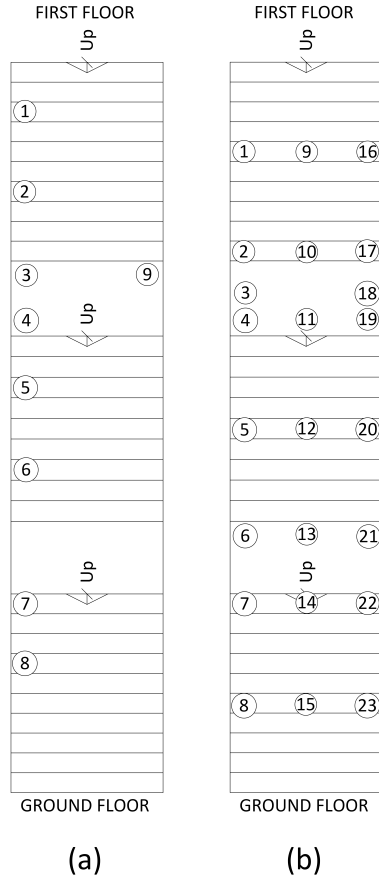
Figure 3: Accelerometer mesh for the staircase: original mesh (a) and extended mesh for the tests related to the multi-reference approach (b).

up by steel and marble) in the Bovisa campus of Politecnico di Milano (see Figure 2a). The second one is the helipad of Palazzo Regione Lombardia, one of the tallest high-rise buildings in Milan [31, 32, 33]. This latter structure is circularly shaped, with a diameter of approximatively 30 m (see Figure 2b).

The layout of the accelerometers used to collect the dynamic response of the two structures are presented in Figures 3a and 4. These accelerometer layouts were employed both in OMA and OMAH tests. The structures were excited in OMAH tests by using the inertial principle: the force was applied by moving a
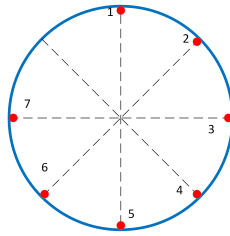
Figure 4: Accelerometer mesh for the helipad.

Table 2: Modal data of the helipad identified by means of OMA

| Mode | $\omega_r/(2\pi)$ [Hz] | $\xi_r$ [%] |
|------|------------------------|-------------|
| 1 | 3.32 | 0.90 |
| 2 | 3.54 | 0.60 |
| 3 | 3.57 | 1.70 |
| 4 | 3.85 | 0.32 |
| 5 | 3.86 | 0.40 |
| 6 | 4.73 | 0.54 |
| 7 | 4.75 | 0.43 |
| 8 | 6.79 | 0.20 |

mass with an actuator laid down on the structure. The actuator was a small electro-dynamic shaker in the case of the staircase and a hydraulic actuator in the case of the helipad. The force exerted was calculated by multiplying the measured value of the mass (3.1 kg for the staircase and 120 kg for the helipad) by its acceleration. The acceleration was measured by using an accelerometer located on the mass (the mass of the accelerometer was in both cases included in the mass used). The amplitudes of the harmonic forces exerted were in the order of 1 N for the staircase and 100 N for the helipad.

The modes excited with such an approach where those having a significant deflection in the vertical direction, which was the working direction of the actuators. Therefore, all the accelerometers depicted in Figures 3a and 4 measure in the vertical direction. As for the helipad, the accelerometers were placed on

the outer edge because the helipad is connected to the ground at its centre; therefore, the vertical mode shapes have their largest components on the outer edge, as also evidenced by the OMA results.

All the signals were acquired by means of a 24 bit analog-to-digital acquisition board with anti-aliasing filters on board. The sampling frequency used was 256 Hz in all the tests. The accelerometers used for acquiring the structural response were low-noise high-sensitivity seismic piezoelectric accelerometers with full scale equal to 4.9 m/s$^2$ and sensitivity equal to 1019.4 mV/(m/s$^2$) (types PCB Piezotronics 393B12 and 393B31). The accelerometers used to measure the acceleration of the mass moved by the actuator were again piezoelectric, but with a higher full scale (49 m/s$^2$) to prevent saturation (PCB Piezotronics 393A03). All the signals were acquired synchronously in a single data set in each test.

In the OMAH tests the structural response was measured during 100 s (in steady state) for the staircase. Indeed, due to the low force provided, the acquisition time was increased in order to improve the accuracy associated to the estimation of the FRFs at $\omega_{\text{ex}}$ [28]. Conversely, data were recorded during 20 s (in steady state) in the case of the helipad thanks to the higher SNRs.

It is noted that the FRFs measured at $\omega_{\text{ex}}$ in OMAH tests are in acceleration over force, and not in displacement over force as those used in Sections 2.1 and 2.2. However, it is trivial to find the FRF in terms of displacement over force by dividing the acceleration FRF by $-\omega_{\text{ex}}^2$.

For the OMA tests, signals were recorded during 1800 s in the case of the staircase and during more than 7200 s in the case of the helipad. The results in terms of eigenfrequencies and non-dimensional damping ratios (identified by means of the polyreference least squares frequency domain method [34]) of the OMA are reported in Table 1 for the staircase and in Table 2 for the helipad. It is noticed that the OMA tests were also useful to find where the mode shapes considered were characterized by significant modal components. This allowed to place the actuator during the OMAH tests in DOFs far from nodes of the modes considered in the given test. More details on the choice of the actuator

14

location will be provided in Section 3.2.

Subsection 3.1 shows that an enhancement of the accuracy of the scaling can be obtained by increasing the number of response DOFs used for scaling. Subsection 3.2 treats the results related to the multi-reference approach with residual terms (see Section 2.2).

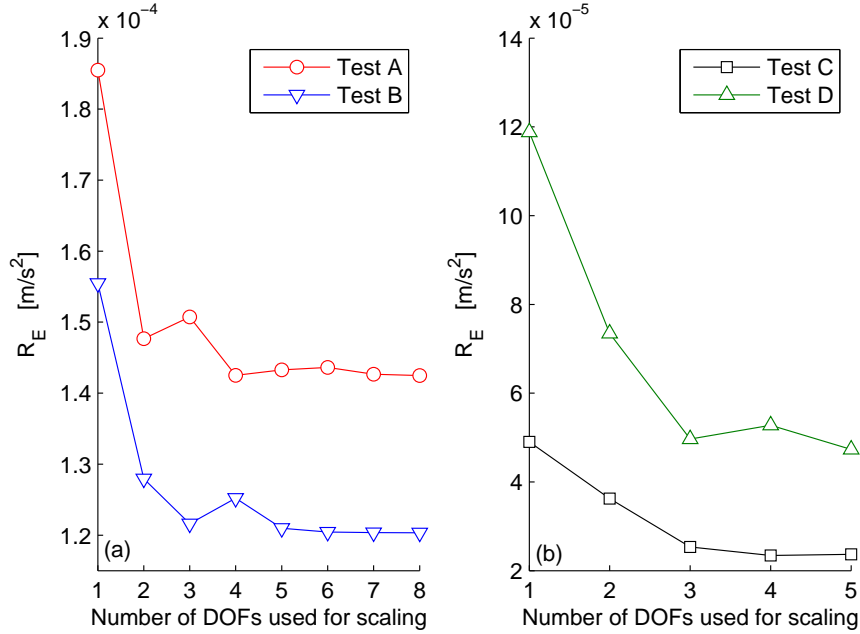## 3.1. Enhancement of accuracy by increasing the number of degrees-of-freedom used for scaling



Figure 5: Plot of the error $R_{\mathrm{E}}$ as function of the number of DOFs used for scaling: tests for the staircase (a) and for the helipad (b). The difference in the size of the error between the two structures is due to the difference in SNR

This section aims at demonstrating that an increase of the number of response DOFs used for scaling results in an improvement of the accuracy of the estimated modal masses.

The OMAH tests carried out are reported in Table 3 for both structures. The column related to the order of DOFs used for scaling in the table refers to

Table 3: Tests carried out for the staircase and the helipad. Refer to Figure 3a and Table 1 for the DOFs and the modes of the staircase, respectively. Refer to Figure 4 and Table 2 for the DOFs and the modes of the helipad, respectively.

| Test ID | structure tested | actuator position (DOF) | $\omega_{\mathrm{ex}}/(2\pi)$ [Hz] | mode excited | order of the DOFs used for scaling |
|---------|------------------|-------------------------|-----------------------------------|--------------|------------------------------------|
| A | staircase | 4 | 8.77 | 2 | 4, 5, 3, 6, 2, 7,1, 8 |
| B | staircase | 9 | 7.75 | 1 | 5, 4, 3, 6, 2, 7,1, 8 |
| C | helipad | 3 | 3.32 | 1 | 3, 4, 5, 6, 7 |
| D | helipad | 6 | 6.53 | 8 | 3, 4, 5, 6, 7 |

the fact that the number of DOFs used for scaling was increased step by step for each test. The DOFs used for scaling the modal model of the staircase were selected in descending mode shape coefficient size. As an example, referring to test A in the table, the scaling was carried out firstly using only DOF 4, then DOFs 4 and 5, then DOFs 4, 5 and 3, and so on. It should be noted that for these tests we did not include the residual terms in Equation (12), as it was found that it was not necessary in this case (the results of the analysis showed negligible changes when considering the residual terms).

In the next step, the acceleration response of each DOF, for a force equal to that applied experimentally, was reconstructed by means of Eq. (5) (multiplied by a term equal to $-\omega_{\mathrm{ex}}^2$ to obtain accelerance format), where the poles and the unscaled eigenvector components came from OMA, while the modal masses from OMAH scaling. This recalculated response will be referred to as *reconstructed response* from here on. The calculation of this reconstructed response allows to calculate an error $E_i$ between the experimental and reconstructed responses for each DOF:

$$E_i = A_{\mathrm{rec}}^i - A_{\mathrm{meas}}^i \tag{13}$$

where $A_{\mathrm{rec}}^i$ is the amplitude of the reconstructed response in the $i^{th}$ DOF and $A_{\mathrm{meas}}^i$ is the amplitude of the measured response in the $i^{th}$ DOF. The amplitude

of the mono-harmonic force applied experimentally and $A^i_{\mathrm{meas}}$ can be estimated with different approaches in either time or frequency domain. In this case a sine-fit procedure in time domain was employed [28].

Then, an error $R_{\mathrm{E}}$ is calculated as:

$$R_{\mathrm{E}} = \sqrt{\frac{\sum_{i=1}^{z} E_i^2}{z}} \tag{14}$$

where $z$ is the total number of DOFs where the structural response was measured, which can be different from (i.e. higher than) the number of DOFs used for scaling, $m$.

Figure 5 shows $R_{\mathrm{E}}$ as a function of the number of DOFs used for scaling, for the tests presented in Table 3. It is evident that when the number of DOFs used for scaling is increased, the accuracy of the whole response estimation improves, even if DOFs with low eigenvector components (e.g. DOFs 1, 7 and 8 of the staircase) are added in the scaling procedure. Therefore, this figure confirms that the increase of the number of DOFs employed for scaling has positive effects. Such an improvement is achieved at a very small additional computational cost and complication of the test procedure.

Interestingly, the results in Figure 5 also indicate that the first few added response DOFs significantly reduce the errors in the modal mass estimates, whereas adding more DOFs contribute less. The results are similar for both structures. A plausible explanation for this may be that, after adding a few DOFs, the statistical errors in the modal mass estimates, that stem from noise in the FRF estimates, are already essentially removed. The remaining errors are then due to (small) errors in the modal parameter estimates.

*3.2. Validation of the multi-reference approach*

This section presents the tests carried out to validate the multi-reference approach, including residual terms. The accelerometer mesh for the staircase was extended compared to the previously mentioned tests. This was necessary for the multi-reference approach. Indeed, an excitation DOF where at least one mode cannot be properly excited is necessary to prove the efficiency of the
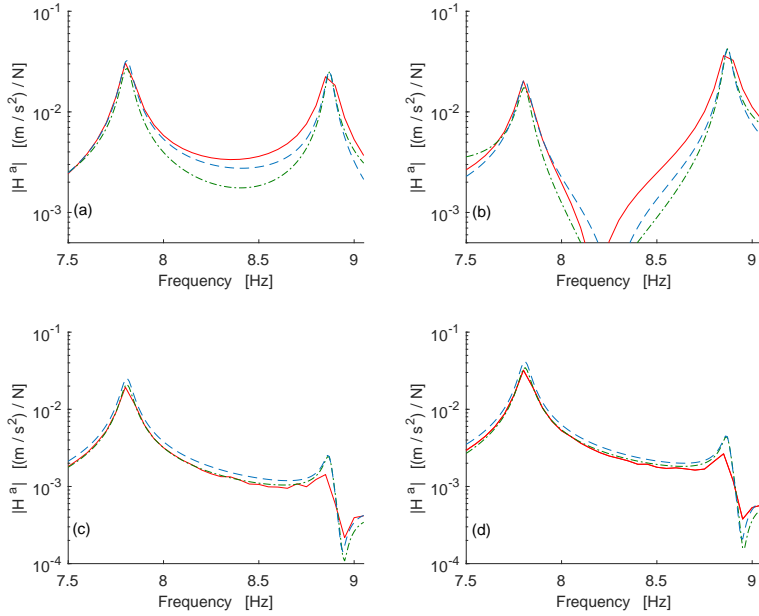
17

Figure 6: $|H^a|$ for the staircase for some DOFs (see Figure 3b) chosen as example: input in DOF 1 and response in DOF 18 (a), input in DOF 1 and response in DOF 3 (b), input in DOF 9 and response in DOF 16 (c), input in DOF 9 and response in DOF 17 (d). Red solid lines for experimental modal analysis results, green dash-dotted lines for the FRFs reconstructed using the method of Section 2.2 (i.e. global scaling), blue dashed lines for the FRFs reconstructed by scaling with a single response DOF.

approach. Cappellini et al. analysed the same staircase [35] and showed that the second mode is characterized by a torsion. This means that the DOFs in the middle of the staircase have low eigenvector components (not perfectly null because the mode is not perfectly symmetric with respect to the longitudinal axis of the staircase). Therefore, a new accelerometer mesh was designed (see Figure 3b) and a new OMA was carried out (see Table 4) before performing the OMAH tests.

As for the helipad, modes 6 and 7 were considered (see Table 2) because they are close to each other in frequency which is a challenging situation appropriate for testing the multiple-reference approach. As for the excitation locations, DOFs 3 and 6 were considered because the OMA results showed that in DOF
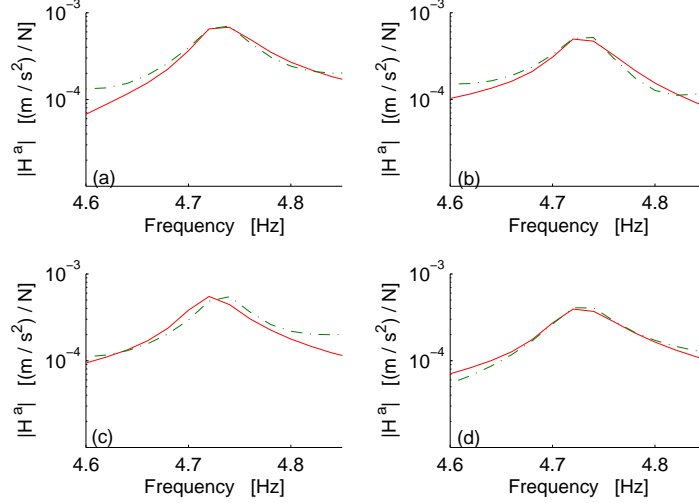
18

Figure 7: $|H^a|$ for the helipad for some DOFs (see Figure 4) chosen as example: input in DOF 3 and response in DOF 3 (a), input in DOF 3 and response in DOF 2 (b), input in DOF 6 and response in DOF 3 (c), input in DOF 6 and response in DOF 7 (d). Red solid lines for experimental modal analysis results, green dash-dotted lines for the FRFs reconstructed using the method of Section 2.2 (i.e. global scaling)

6 the mode shape component of mode 6 is high, while that of mode 7 is lower. The OMAH tests carried out are reported in Table 5 for both the structures.

Since several modes are taken into account in these tests, the index $R_\mathrm{E}$ defined previously cannot be used to describe the accuracy of the scaling procedure. Therefore, experimental and reconstructed FRFs will be used for assessing the accuracy of the scaling procedure. Reconstructed FRFs are those recalculated in the frequency range of the modes considered after finding the modal

Table 4: Modal data of the staircase identified by means of the new OMA with the accelerometer mesh of Figure 3b.

| Mode | $\omega_r/(2\pi)$ [Hz] | $\xi_r$ [%] |
|------|------------------------|-------------|
| 1    | 7.81                   | 0.36        |
| 2    | 8.87                   | 0.24        |

19

Table 5: Tests carried out for the staircase and the helipad. Refer to Figure 3b and Table 4 for the DOFs and the modes of the stair, respectively. Refer to Figure 4 and Table 2 for the DOFs and the modes of the helipad, respectively.

| Structure tested | Actuator positions (DOFs) | Modes considered | $\omega_{\mathrm{ex}}/(2\pi)$ [Hz] | DOFs used for scaling |
|---|---|---|---|---|
| Staircase | 1 and 9 | 1 and 2 | 7.75, 7.80, 7.86, 8.85, 8.90, 8.95 | 1, 2, 3, 4, 5, 9, 10, 11, 12, 16, 17, 18, 19, 20 |
| Helipad | 3 and 6 | 6 and 7 | 4.65, 4.69, 4.73, 4.74, 4.77, 4.80 | all (i.e., from 1 to 7) |

masses with multi-reference OMAH, taking into account the residual terms due to out-of-band modes. This required to have experimental FRFs to be used as reference. For the staircase, the shaker used for OMAH tests was employed to provide random excitation to the structure and estimate its FRFs. The actuator was able to provide excitation by moving a mass, as described previously. The shaker was placed in the DOFs taken into account to provide excitation during OMAH. Random noise was then used to excite the structure, and the FRFs were estimated with the $H_1$ estimator [36]. The coherence was close to unity in the frequency range around the two first natural frequencies of the staircase. For the helipad, a similar approach was employed. Here, a hydraulic actuator was used in place of the electro-dynamic shaker, as mentioned above. Furthermore, stepped-sine excitation [36] was preferred to random excitation in order to improve the accuracy of the experimental FRFs.

Figures 6 and 7 show some comparisons between experimental (red solid lines) and reconstructed (green dash-dotted lines) FRFs for the staircase and the helipad, respectively. These FRFs are expressed in terms of acceleration over force (indicated as $H^{\mathrm{a}}$) in order to directly show the measured reference FRFs. The proposed method is evidently able to properly scale the modes and to reconstruct the FRFs. Indeed, the reconstructed FRFs satisfactorily match the reference experimental FRFs. Sometimes, differences between experimental and reconstructed FRFs can be noticed far from the resonances (e.g. plot (b) of

Fig. 6 and plot (a) of Fig. 7). These differences are mainly due to biased OMA results (both poles and unscaled mode shape coefficients). As an example, the damping of the second mode in Fig. 6 is slightly underestimated.

Tables 6 and 7 show the modal mass values estimated by means of three different approaches: (i) with experimental modal analysis (EMA) using the measured FRFs, (ii) employing the OMAH method with global scaling, and also (iii) using the OMAH method with the scaling carried out using a single response DOF. Considering this last approach, for the helipad response DOF 3 was used (employing the co-located FRF); as for the staircase, response DOF 3 was used (employing the FRF obtained by exciting in DOF 1). The modal masses are calculated so that the same mode shape coefficient is scaled to 1 for all the three methods in order to have a straightforward comparison. It is evident that moving from a scaling procedure using a single DOF to the global scaling, the estimated modal masses become closer to those found with EMA. Furthermore, Figs. 6c and d show that the use of a single response DOF for scaling leads to overestimation in the first resonance peak, while the global scaling does not cause such a problem because it works on many DOFs.

The accuracy of the OMAH method is difficult to accurately deduct, since the size of the contributions to errors are largely unknown. The following causes may contribute to the inaccuracy of the modal mass estimates:

- errors in the estimates of the complex amplitudes of force and responses used to compute the FRF values, which include sensor inaccuracies plus the uncertainty in the three-parameter sine fit,

- errors in the mode shape coefficients from the OMA, also affected by the sensor inaccuracies plus errors in parameter estimation, and

- errors in the pole estimates from the OMA, largely originating from the parameter estimation process and less affected by errors in sensors.

An additional cause of error in the comparisons between EMA and OMA in the present Section, could furthermore be a difference in the measurement lo-

cations, since we compare results from different measurement occasions. Since the errors in mode shape coefficients are unknown and depend on the quality of the measurements and the OMA parameter estimation, it is very difficult to estimate any absolute uncertainty of the modal masses. We attribute the differences between the modal masses from EMA and OMAH (global scaling) observed in Tables 6 and 7 mainly to biased OMA results, since the synthesized FRFs based on the EMA model agreed very well with the measured FRFs. It should be noted that each accelerometer in the EMA measurements as well as in the OMA measurements has an inaccuracy of minimum $\pm 5$ % (perhaps more, since the IEPE sensors we used have larger error in the low frequency range). Adding errors from the OMA parameter estimation, a total error of $\pm 20$ % is likely. Comparing the results between EMA and OMAH with global scaling in Tables 6 and 7, shows that the difference in modal mass estimates for the staircase are 8 % and 40 % for the two modes, respectively, and for the helipad the differences are approx. 20 % for both modes. Statistically, the values are thus consistent with approximately $\pm 20$ % error in the modal mass estimates in the worst case for mode two of the staircase, and half of that for the helipad. By looking closely at the results, it turns out that the damping of the OMA analysis of the second mode of the staircase is unreliable and most likely too small, which may be the cause of the larger error for this mode. Finally, it should be noted that a desirable feature of the OMAH method is that it allows the obtained accuracy of the scaling of the modal model to be assessed by comparing the measured harmonic response in the different response DOFs with computated values of the response using the excitation force and the FRF between the two points computed from the modal model, as discussed in Section 3.1. This is an advantage of the OMAH method over other methods such as using a FE model mass matrix or repeated OMA analyses with different mass configurations, for which no such assessment can be made.

Table 6: Values of the modal mass $m_r$ for the three different ways used to estimate them (staircase).

| mode number | $m_r$ with EMA | $m_r$ with OMAH (global scaling) | $m_r$ with OMAH (just 1 DOF used for scaling) |
|---|---|---|---|
| 1 (at 7.81 Hz) | $1.67{\cdot}10^3$ | $1.54{\cdot}10^3$ | $1.28\ {\cdot}10^3$ |
| 2 (at 8.87 Hz) | $1.31{\cdot}10^3$ | $1.85{\cdot}10^3$ | $1.83{\cdot}10^3$ |

Table 7: Values of the modal mass $m_r$ for the three different ways used to estimate them (helipad).

| mode number | $m_r$ with EMA | $m_r$ with OMAH (global scaling) | $m_r$ with OMAH (just 1 DOF used for scaling) |
|---|---|---|---|
| 6 (at 4.73 Hz) | $2.03{\cdot}10^5$ | $1.64{\cdot}10^5$ | $2.87{\cdot}10^5$ |
| 7 (at 4.75 Hz) | $2.32{\cdot}10^5$ | $1.89{\cdot}10^5$ | $1.60{\cdot}10^5$ |

## 4. Conclusions

This paper has dealt with further development of the OMAH method for scaling the unscaled mode shapes obtained by means of operational modal analysis. The method requires to carry out tests with mono-harmonic excitation at (or close to) eigenfrequencies of the structure.

Particularly, the paper treats two different topics. First, it explains how to increase the accuracy of the scaling procedure. This is accomplished by increasing the number of response degrees-of-freedom used in the scaling procedure. The optimal amount of DOFs to be added for increasing the accuracy of the scaling is not straightforward to calculate. Indeed, it depends on many factors, such as: error on each modal component used, value of each modal component, and so on. However, even the use of two or three DOFs for scaling allows to improve accuracy, as demonstrated in the paper. The experimental results also suggests that the first few added response DOFs contribute most to the reduced variance in the modal mass estimates, adding more DOFs then results in less improvement. It is plausible that this is due to the fact that a few additional DOFs are enough to eliminate the random error due to noise in the measure-

ments. After this is accomplished, the remaining error is a bias error, due to the errors in the modal parameters.

Second, the OMAH method is extended to the case of multiple references, thus making OMAH as general as possible and applicable to any possible practical case. The global scaling formulation, developed in the paper, has the particular advantage of being able to handle cases where one single DOF cannot be found, in which the mode shape coefficients, for all modes to be scaled, are high. Excitation can then instead be applied in different locations for the different modes to be scaled. The procedure proposed also allows to take into account residual terms accounting for modes outside of the range of modes to be scaled. It is recommended to always include these parameters, to ensure that the matrix built up of mode contributions is well conditioned.

The presented approach can be considered as the analogue of global parameter estimation in the classical experimental modal analysis.

The analytical procedures described in the paper were validated by means of experimental tests on two different structures: a staircase and a helipad. In both cases, the results of the tests were satisfactory, demonstrating the reliability of the global scaling method proposed in the paper.

### Acknowledgements

### References

[1] A. Cigada, A. Caprioli, M. Redaelli, M. Vanali, Vibration testing at meazza stadium: Reliability of operational modal analysis to health monitoring purposes, Journal of Performance of Constructed Facilities 22 (4) (2008) 228–237.

[2] G. H. James, T. G. Carne, J. P. Lauffer, The natural excitation technique (next) for modal parameter extraction from operating structures, Modal

Analysis-the International Journal of Analytical and Experimental Modal Analysis 10 (4) (1995) 260–277.

[3] F. Ubertini, C. Gentile, A. Materazzi, Automated modal identification in operational conditions and its application to bridges, Engineering Structures 46 (2013) 264–278.

[4] C. Rainieri, G. Fabbrocino, Development and validation of an automated operational modal analysis algorithm for vibration-based monitoring and tensile load estimation, Mechanical Systems and Signal Processing 60–61 (2015) 512–534.

[5] C. Devriendt, P. Guillaume, Identification of modal parameters from transmissibility measurements, Journal of Sound and Vibration 314 (1-2) (2008) 343–356.

[6] T. Wang, O. Celik, F. Catbas, L. Zhang, A frequency and spatial domain decomposition method for operational strain modal analysis and its application, Engineering Structures 114 (2016) 104–112.

[7] E. Parloo, P. Verboven, P. Guillaume, M. Van Overmeire, Sensitivity-Based Operational Mode Shape Normalisation, Mechanical Systems and Signal Processing 16 (5) (2002) 757–767. doi:10.1006/mssp.2002.1498.

[8] E. Parloo, B. Cauberghe, F. Benedettini, R. Alaggio, P. Guillaume, Sensitivity-based operational mode shape normalisation: Application to a bridge, Mechanical Systems and Signal Processing 19 (1) (2005) 43–55. doi:10.1016/j.ymssp.2004.03.009.

[9] D. Bernal, Modal Scaling from Known Mass Perturbations, Journal of engineering mechanics 130 (9) (2004) 1083–1088. doi:10.1061/(ASCE)0733-9399(2004).

[10] D. Bernal, A receptance based formulation for modal scaling using mass perturbations, Mechanical Systems and Signal Processing 25 (2) (2011)

621–629. doi:10.1016/j.ymssp.2010.08.004.

URL `http://dx.doi.org/10.1016/j.ymssp.2010.08.004`

[11] G. Coppotelli, On the estimate of the FRFs from operational data, Mechanical Systems and Signal Processing 23 (2) (2009) 288–299. doi:10.1016/j.ymssp.2008.05.004.

[12] M. Lopez-Aenlle, P. Fernandez, R. Brincker, A. Fernandez-Canteli, Scaling-factor estimation using an optimized mass-change strategy, Mechanical Systems and Signal Processing 24 (5) (2010) 1260–1273. doi:10.1016/j.ymssp.2009.06.011.

[13] M. Lopez-Aenlle, R. Brincker, F. Pelayo, A. F. Canteli, On exact and approximated formulations for scaling-mode shapes in operational modal analysis by mass and stiffness change, Journal of Sound and Vibration 331 (3) (2012) 622–637. doi:10.1016/j.jsv.2011.09.017.

[14] R. Brincker, P. Andersen, A Way of Getting Scaled Mode Shapes in Output Only Modal Testing, in: International Modal Analysis Conference (IMAC) - 3-6 February 2003, Orlando (USA), 2003.

[15] R. Brincker, J. Rodrigues, P. Andersen, Scaling the Mode Shapes of a Building Model by Mass Changes, in: International Modal Analysis Conference (IMAC) - 26-29 January 2004, Dearborn (USA), 2004.

URL `http://www.svibs.com/solutions/literature/2004_2.pdf`

[16] M. López-Aenlle, R. Brincker, A. F. Canteli, Some Methods to Determine Scaled Mode Shapes in Natural Input Modal Analysis, in: International Modal Analysis Conference (IMAC) - January 31-February 3 2005, Orlando (USA), 2005, pp. 1–11.

[17] P. Fernández, M. Lopez-Aenlle, L. Garcia, R. Brincker, Scaling Factor Estimation Using an Optimized Mass Change Strategy . Part 1 : Theory, in: International operational modal analysis conference (IOMAC) - April 30-May 2 2007, Copenhagen (Denmark), 2007.

[18] L. Yu, H. Song, Scaling mode shapes in output-only structure by a mass-change-based method, Shock and Vibration 2017 (2017) Article ID 2617534.

[19] M. Khatibi, M. Ashory, A. Malekjafarian, R. Brincker, Mass–stiffness change method for scaling of operational mode shapes, Mechanical Systems and Signal Processing 26 (2012) 34–59.

[20] J. Cara, Computing the modal mass from the state space model in combined experimentaloperational modal analysis, Journal of Sound and Vibration 370 (2016) 94–110. doi:10.1016/j.jsv.2016.01.043.

[21] E. Reynders, D. Degrauwe, G. De Roeck, F. Magalhães, E. Caetano, Combined Experimental-Operational Modal Testing of Footbridges, Journal of Engineering Mechanics 136 (6) (2010) 687–696. doi:10.1061/(ASCE)EM.1943-7889.0000119.

[22] J. S. Hwang, H. Kim, J. Kim, Estimation of the modal mass of a structure with a tuned-mass damper using H-infinity optimal model reduction, Engineering Structures 28 (1) (2006) 34–42. doi:10.1016/j.engstruct.2005.06.022.

[23] J. M. W. Brownjohn, A. Pavic, Experimental methods for estimating modal mass in footbridges using human-induced dynamic excitation, Engineering Structures 29 (11) (2007) 2833–2843. doi:10.1016/j.engstruct.2007.01.025.

[24] J. A. Porras, J. De Sebastian, C. M. Casado, A. Lorenzana, Modal mass estimation from output-only data using oscillator assembly, Mechanical Systems and Signal Processing 26 (1) (2012) 15–23. doi:10.1016/j.ymssp.2011.06.015.
URL http://dx.doi.org/10.1016/j.ymssp.2011.06.015

[25] W. A. Smith, R. B. Randall, Cepstrum-based operational modal analysis revisited: a discussion on pole-zero models and the regeneration of frequency response functions, Mechanical Systems and Signal Processing 79 (2016) 30–46.

[26] M. López-Aenlle, R. Brincker, Modal scaling in operational modal analysis using a finite element model, International Journal of Mechanical Sciences 76 (2013) 86–101.

[27] A. Brandt, M. Berardengo, S. Manzoni, A. Cigada, Harmonic scaling of mode shapes for operational modal analysis, in: International Conference on Noise and Vibration Engineering (ISMA), September 17-19, Leuven, Belgium, 2016.

[28] A. Brandt, M. Berardengo, S. Manzoni, A. Cigada, Scaling of mode shapes from operational modal analysis using harmonic forces, Journal of Sound and Vibration 407 (2017) 128–143. doi:10.1016/j.jsv.2017.06.033.

[29] A. Brandt, M. Berardengo, S. Manzoni, A. Cigada, Using three–parameter sine fitting for scaling mode shapes with OMAH, in: the 7th International Operational Modal Analysis Conference (IOMAC), Ingolstadt, Germany, May 10 − 12, 2017.

[30] A. Brandt, M. Berardengo, S. Manzoni, M. Vanali, A. Cigada, Global scaling of oma modes shapes with the omah method, in: International Conference on Structural Engineering Dynamics (ICEDYN), Ericeira, Portugal, July 3 − 5, 2017.

[31] G. Busca, A. Cigada, E. Mola, F. Mola, M. Vanali, Dynamic testing of a helicopter landing pad: Comparison between operational and experimental approach, Journal of Civil Structural Health Monitoring 4 (2) (2014) 133–147.

[32] A. Cigada, E. Mola, F. Mola, G. Stella, M. Vanali, Dynamic behavior of the palazzo lombardia tower: Comparison of numerical models and experimental results, Journal of Performance of Constructed Facilities 8 (3) (2014) 491–501.

[33] M. Berardengo, G. Busca, S. Grossi, S. Manzoni, M. Vanali, The monitoring

of palazzo lombardia in milan, Shock and Vibration 2017 (2017) Article ID 8932149. doi:10.1155/2017/8932149.

[34] C. Rainieri, G. Fabbrocino, Operational Modal Analysis of Civil Engineering Structures, Springer New York, 2014.

[35] A. Cappellini, S. Manzoni, M. Vanali, A. Cigada, Evaluation of the dynamic behaviour of steel staircases damped by the presence of people, Engineering Structures 115 (2016) 165–178. doi:10.1016/j.engstruct.2016.02.028.

[36] A. Brandt, Noise and Vibration Analysis – Signal Analysis and Experimental Procedures, John Wiley and Sons, 2011.